Journal of
MATERIALS RESEARCH

Chemical attachment of organic functional groups to single-walled carbon nanotube material

Y. Chen and R. C. Haddon
Departments of Chemistry and Physics, University of Kentucky, Lexington, Kentucky 40506-0055

S. Fang, A. M. Rao, and P. C. Eklund
Department of Physics and Astronomy, University of Kentucky, Lexington, Kentucky 40506-0055

W. H. Lee, E. C. Dickey, and E. A. Grulke
Department of Chemical and Materials Engineering, University of Kentucky, Lexington, Kentucky 40506-0055

J. C. Pendergrass, A. Chavan, and B. E. Haley
Departments of Chemistry and Pharmacy, University of Kentucky, Lexington, Kentucky 40506-0055

R. E. Smalley
Center for Nanoscale Science and Technology, Rice Quantum Institute and Departments of Chemistry and Physics, Rice University, Houston, Texas 77251

(Received 6 February 1998; accepted 3 May 1998)

We have subjected single-walled carbon nanotube materials (SWNTM's) to a variety of organic functionalization reactions. These reactions include radioactive photolabeling studies using diradical and nitrene sources, and treatment with dichlorocarbene and Birch reduction conditions. All of the reactions provide evidence for chemical attachment to the SWNTM's, but because of the impure nature of the staring materials, we are unable to ascertain the site of reaction. In the case of dichlorocarbene we are able to show the presence of chlorine in the SWNT bundles, but as a result of the large amount of amorphous carbon that is attached to the tube walls, we cannot distinguish between attachment of dichlorocarbene to the walls of the SWNT's and reaction with the amorphous carbon.

I. INTRODUCTION

While present single-walled nanotube (SWNT) studies are focused on the as-prepared, pristine, and doped materials,[1–3] if the SWNT's are to achieve their full potential, it will be necessary to bring about chemical modification of the basic structure. The ability to disperse and perhaps dissolve the SWNT's would greatly improve the prospects for processible materials that can be aligned and formed into useful structures. Chemical functionalization would be an important step in this direction as well as opening up interesting opportunities in its own right. If it were possible to chemically modify the surface of the nanotube in a controlled manner, this would afford a number of opportunities for tailoring the structural and electronic properties.

It is important to distinguish the functionalization that is proposed here from the type of chemistry that is usually carried out on graphite. For example, it is well known that under sufficiently forcing conditions, graphite will undergo fluorination and oxidation processes that lead to almost completely saturated structures. In this way, most of the interesting electronic properties of graphite are lost. What is required here, is a reagent that will selectively attack a few of the π-bonds in a controlled manner without bringing about a total destruction of the graphene electronic structure of the SWNT.

It is well known that the chemistry of the fullerenes is characterized by addition reactions.[4–8] The fullerenes undergo such reactions with relative ease because the conversion of trigonal carbon atoms to tetrahedral carbon atoms serves to release the tremendous strain present in the spheroidal geometry.[9] It is straightforward to understand how σ-bond formation will be assisted by the geometry of the carbon atoms by a consideration of the pyramidalization angle (θ_P), which is directly related to the curvature at a conjugated carbon atom.[10] As may be seen in Scheme 1, the C_{60} pyramidalization angle of $\theta_P = 11.64°$ is actually closer to the ideal tetrahedral angle than to the planar geometry required for trigonal hybridization.

Thus, it is not surprising to find that the sites of preferential reactivity in carbon nanotubes are at the caps where the pyramidalization and curvature is greatest, and comparable in magnitude to that of the fullerenes.[11] Pioneering studies by a number of workers used this preferential reactivity to open the caps of carbon nano-

https://doi.org/10.1557/JMR.1998.0337

tubes and allow various species to be admitted to the interior galleries of the tubes.[12–15] While this is a particularly interesting approach to nanotube chemistry, the nondestructive attachment of functional groups to the walls of the nanotubes presents a further challenge to experiment, because the reduced strain in the walls lessens the normal fullerene reactivity. The chemical reactions that selectively attack the nanotube ends are not satisfactory for the production of processable materials, because this type of transformation is simply too localized to bring about the necessary change in bulk properties of materials with the high aspect ratio of the (10,10) SWNT's.[16]

The metallic (10,10) SWNT's are interesting objects for surface chemistry. The idea of chemically modifying a metal by controlled chemistry presents an interesting challenge, because as metals they have zero band gap, and thus are predicted to be extremely reactive in simple theories.[17] The reason that the SWNT's are not very reactive may be traced to the low value of the density of states at the Fermi level in the metallic SWNT's coupled with the fact that bond formation is necessarily local.

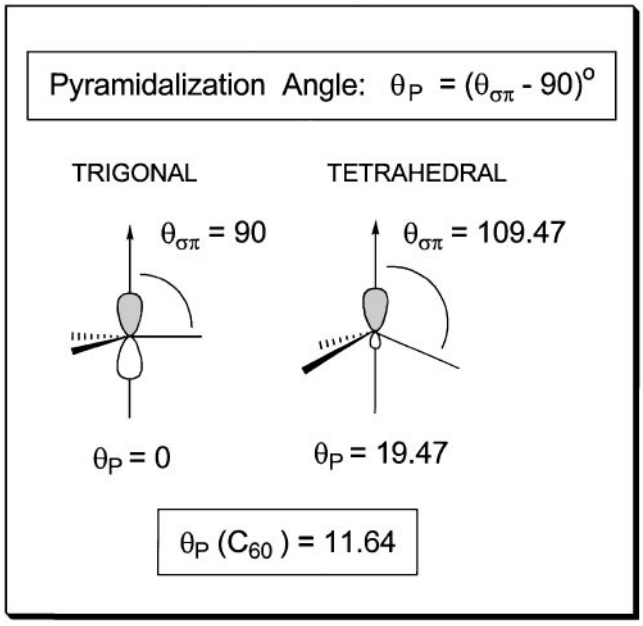

SCHEME 1.

Furthermore, the curvature in the nanotube walls is much less than in the fullerenes and so strain relief does not offer the same driving force for chemical reactivity that is experienced by the fullerenes. For example, in the (10,10) SWNT's the pyramidalization angle is $\theta_P = 3.01°$, compared to $\theta_P = 11.64°$ in C_{60}. Hence, the local strain per carbon atom due to curvature is 0.5_4 kcal/mol [(10,10) SWNT] and 8.1 kcal/mol (C_{60}). This local strain energy (together with a global strain component) is completely relieved when the fullerenes undergo addition reactions, and it is this factor that is largely responsible for their reactivity.[9] The (10,10) SWNT's will receive a much smaller local strain relief on reaction, although they may also obtain a component of global strain relief as the other atoms in the wall relax.

It is important to note that the above arguments apply to perfect SWNT's. In the event that the sample contains highly stressed, bent, or defective SWNT's,[1,18] it may well be possible to use the pyramidalized sites that have high local strain to begin to induce chemical reactions of the type discussed below. Once initiated on the wall of the SWNT, chemical reaction may well become easier in adjacent partial double bonds that will be more localized than those in the body of the SWNT, which are expected to be fully delocalized. Furthermore, if hemispherical fullerene endcaps initiate the growth of the SWNT,[11,16] these fullerene endcaps may serve to initiate reaction, which again could spread to the body of the SWNT.

A depiction of a small piece of the wall of a SWNT is given below in obvious notation (where the arrow represents the direction of propagation of the nanotube).

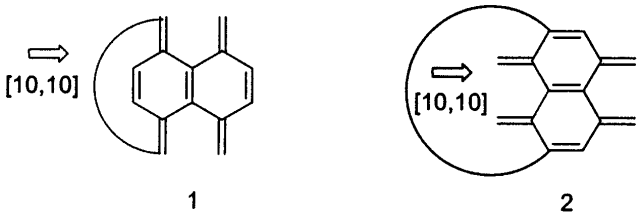

SCHEME 2.

Structures 1 and 2 represent the "armchair" and "zigzag" forms of the (10,10) SWNT's. Strong arguments have been given in favor of the armchair form due to the likely growth mechanism,[16] and we focus on this structure. It is important to note that these Kekule structures consist of just one of the many possible resonance forms.

We exemplify the chemistry that is attempted in this paper, by the addition of dichlorocarbene to armchair (10,10) SWNT.

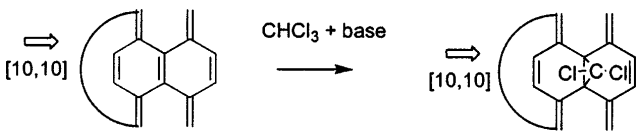

SCHEME 3.

Dichlorocarbene is an electrophilic reagent that adds to deactivated double bonds, but not to benzene[19,20] Similar reactions have been reported for the fullerenes.[21,22] We also report the interaction of SWNT's with other highly reactive synthetic intermediates, with a view to inducing similar chemistry.

II. RESULTS

We made use of SWNT's obtained from two sources in our studies. In both cases the materials are known to grow as ropes which consist of a two-dimensional triangular array of nanotubes. Although the samples contain a substantial fraction of armchair (10,10) SWNT's,[16] there is some spread in tube diameters[23] and in the chiral angle[24,25] of these materials.

A. Single-walled nanotube material obtained by laser ablation[16] (Rice University) referred to as SWNTM1[16]

The reported yield of this process is 70 to 90% SWNT's, and our own high-resolution transmission electron microscopy (HRTEM) studies confirm this value.

B. Single-walled nanotube material obtained from electric-arc discharge[26] (University of Kentucky) referred to as SWNTM2

The reported yield of this process is 80% SWNT's,[26] but in our experiment the yield was about 30–50%.

Bulk studies are greatly hindered by impure starting materials. In addition to the nanoparticles, residual catalyst, and amorphous carbon in SWNTM1 and SWNTM2, we also identified graphite in the SWNTM2 material. All of the studies reported in this paper we carried out on as-received, unpurified materials. A layer of amorphous carbon may be seen to cover a substantial fraction of the surface of the SWNT's in HRTEM, and the presence of this material in intimate contact with the SWNT bundles considerably complicated our analysis of the chemical reaction products. Thus, while we hoped to carry out chemistry on the walls of the SWNT's, we are unable to rule out competing reactions with extraneous material in the samples. Recognizing the heterogeneous nature of the starting materials used in the chemical reactions, we refer to it as single-walled nanotube material (SWNTM).

C. Photolabeling

We began by testing the reactivity of the SWNTM's using photolabeling.[27–29] This technique uses photoactive compounds that generate highly reactive intermediates when exposed to an activating light source. Radiolabeled photoactive compounds allow ready detection of chemical reaction because the radioactive precursor will become incorporated in the target substrate if functionalization has occurred. Such techniques are used routinely in biological applications and are known to be extremely sensitive to incorporation of the radioactive group into the target material. We chose photoactive precursors that would lead to the benzophenone diradical and phenyl nitrene intermediates, in the hope that we could induce the type of chemistry discussed above. The former reagent often reacts by proton abstraction,[27] but there is precedent in the literature for photocycloaddition to give oxetanes.[30] Nitrenes are sufficiently reactive to add to benzene, and perfluorophenyl azides can be used to photochemically modify the surface of graphite.[31]

The SWNTM material was suspended in buffer, sonicated, and vortexed and then treated with [γ^{32}P]-benzophenone-ATP or [γ^{32}P]2N_3ATP solution. The mixture was photolyzed at 2354 nm for 15 min and then centrifuged to allow the removal of the unbound photoprobe. The nanotube sample was repeatedly washed and the extracts and nanotubes assayed with a scintillation counter. The results are presented in the form of bar graphs that show the radiation count of the washings and the washed nanotubes.

Figures 1(a) and 1(b) show the results of photolabeling studies on SWNTM1 samples using [γ^{32}P]-benzophenone-ATP and [γ^{32}P]2N_3ATP, respectively, run in methanol suspension. In these two experiments the photoprobe is still visible in the fourth wash, but also in the washed SWNTM's. Of particular note is the observation that almost as much of the probe molecules become attached in the absence of photolysis. Therefore, other mechanisms of attachment are operative, beside the photochemical route.

These studies indicate that the radioactive probes do become attached to the SWNTM material, but do not demonstrate the mode of addition, or if indeed the attachment is chemical or physical. We therefore decided to explore bulk synthesis of chemically modified SWNTM's.

D. Functionalization reactions

Dichlorocarbene is an electrophilic reagent that adds to deactivated double bonds, but not to benzene.[19,20] In this case we hoped to produce the chemistry discussed above (similar reactions have been reported for the fullerenes).[21,22] In a typical experiment, 25 mg of SWNTM's were suspended in a chloroform, water mixture in the presence of a phase transfer catalyst and sonicated. At this point the mixture was cooled, sodium hydroxide added, and the reaction was stirred overnight. The SWNTM's were collected on a nylon membrane after an aqueous workup.

Chemical analysis of the samples showed about 5% chlorine in SWNTM1 and SWNTM2 samples that were exposed to the reaction conditions. The C, H, and

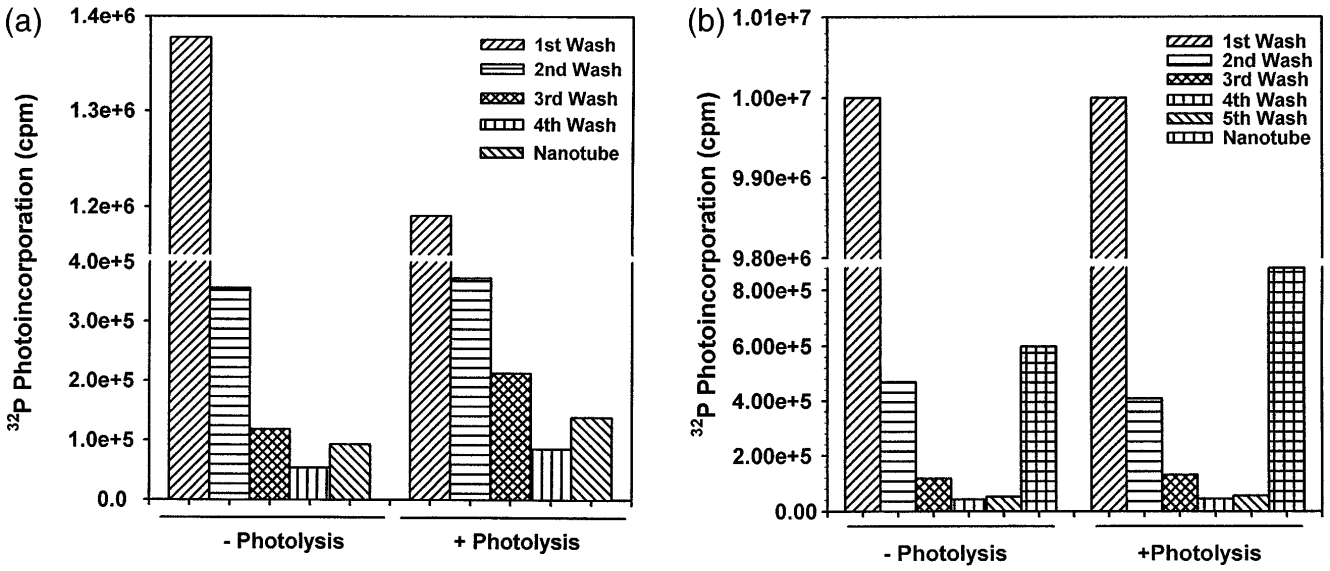

FIG. 1. (a) [^{32}P]benzophenone photolabeling of SWNTM in methanol and a control experiment without photolysis (SWNTM1). (b) [^{32}P]2N$_3$ATP photolabeling of SWNTM in methanol and the control experiment without photolysis (SWNTM1).

Cl analysis accounted only for about two-thirds of the sample mass.

Birch reduction will efficiently hydrogenate benzenoid ring systems, and this was one of the first reactions to be carried out on C_{60}.[32] Thus we subjected samples of SWNTM's to prolonged reduction under Birch conditions. We carried out the reactions under two sets of conditions: (a) refluxing ammonia solution, and (b) in ethylenediamine solution at 100 °C. The latter reaction conditions lead to the incorporation of nitrogen into the sample.

E. Scanning electron microscopy (SEM), energy-dispersive x-ray analysis (EDS), and x-ray photoelectron spectroscopy (XPS) of the products of the dichlorocarbene reaction

The SEM image showed the presence of SWNT's after the reaction. The sample appeared little changed, but the isolation procedure seemed to slightly increase the fraction of SWNT's over the extraneous material.

We analyzed the reacted SWNTM using energy-dispersive x-ray analysis and identified chlorine in the product (Fig. 2). All of our samples showed the oxygen peak that is visible in Fig. 2. The gold peak originated from the coating that was applied for SEM imaging. The chlorine peak was present in material obtained from reactions carried out on SWNTM1 and SWNTM2 samples, and could not be removed by washing.

XPS analysis of the chlorine region (Fig. 3) showed a peak at 201.4 eV from Cl($2p$)—this binding energy (BE) is typical of chlorine in an organic C–Cl bond. Argon ion etching of the sample removes the chlorine peak, suggesting that the chlorine is localized at the surface.

The carbon C($1s$) XPS spectrum of the pristine SWNTM shows a peak at 285 eV for the sp^2 hybridized carbon atoms [Fig. 4(a), narrow peak]. This value is comparable to the C($1s$) BE in graphite (284.5 eV). After reaction with dicholorocarbene, a new strong peak appears in the XPS spectrum of carbon at higher BE [287.5 eV, Fig. 4(b), broad peak]. This BE is typical for C($1s$) ionization of sp^3 carbon in organic chlorocarbons. For example, C*HCl$_3$, 289.6 eV, (—CH$_2$–C*HCl—)$_x$, 286.5 eV.

Figure 4(b) shows the effect of argon ion etching on a sample that had been subject to the dichlorocarbene reaction. The ion etch reduces the intensity of the peak at 287.5 eV while increasing the intensity of the peak at

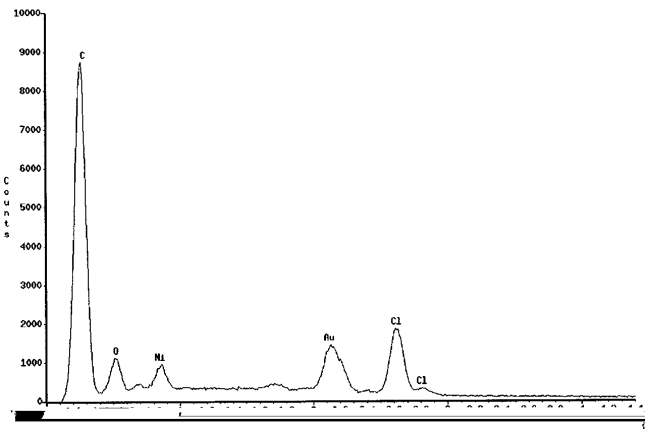

FIG. 2. Low resolution EDS of the SWNTM after dichlorocarbene reaction (SWNTM2; SWNTM1 samples gave similar results).

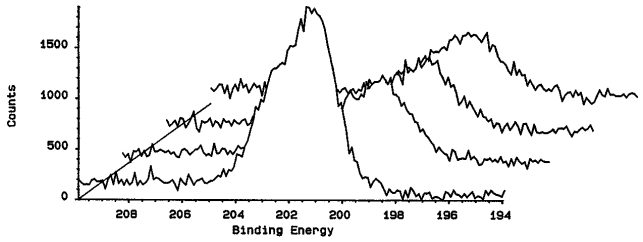

FIG. 3. Chlorine ($2p$) XPS of the SWNTM after the dichlorocarbene reaction (SWNTM2; SWNTM1 samples gave similar results). The background spectra show the effect of argon ion etching.

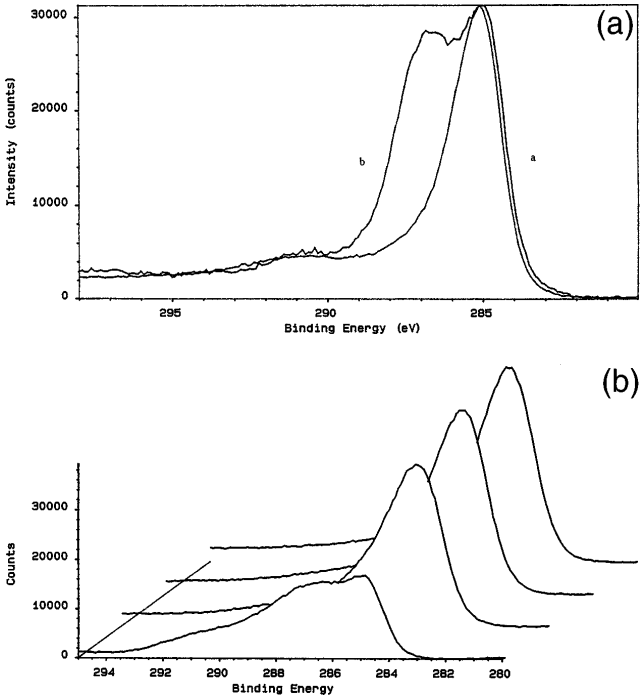

FIG. 4. (a) Carbon ($1s$) XPS of the pristine SWNTM [(a) narrow peak at 285 eV]. (SWNTM2; SWNTM1 sample gave similar result.) The broad peak (b) is from the spectrum taken after reaction with dichlorocarbene. (b) Carbon ($1s$) XPS of the SWNTM after the dichlorocarbene reaction (SWNTM2; SWNTM1 sample gave similar results). The background spectra show the effect of argon ion etching.

285 eV which is characteristic of the pristine SWNTM. Thus, from the standpoint of the XPS spectrum, the etching procedure returned the chemically treated SWNTM sample to a close approximation of its as-prepared state. This suggests that the chemical treatment has modified the surface of the sample without disrupting the SWNT bundles.

Figure 5(a) shows the condensed probe EDS spectrum obtained from a single SWNT rope after the material had been reacted with dichlorocarbene (the Cu signal originates from the grid used to mount the sample). Figure 5(b) shows the EDS spectrum obtained from a catalyst nanoparticle in the same reaction product. The spectra show that dichlorocarbene moities become attached to the SWNT's but not to the catalyst nanoparticles.

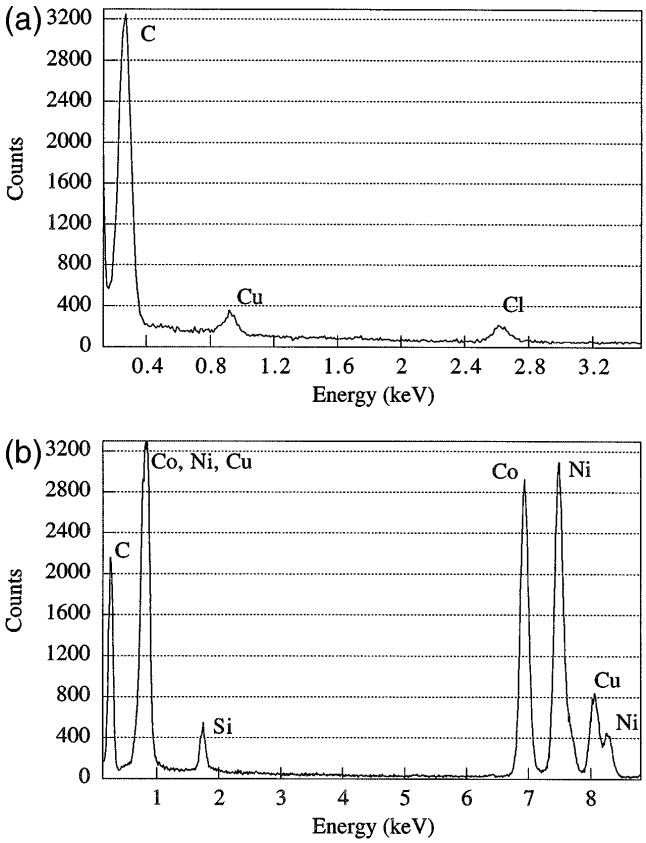

FIG. 5. (a) High resolution EDS of an individual SWNT bundle after dichlorocarbene reaction (SWNTM1). The copper peaks are from the support. (b) High resolution EDS of a catalyst nanoparticle after dichlorocarbene reaction (SWNTM1). The copper peaks are from the support.

We carried out a number of control experiments to eliminate the more obvious sources of contamination. The membranes used for the filtration showed no chlorine peak in the EDS/XPS spectra. Likewise, SWNTM's treated under the same reaction conditions, but in the absence of sodium hydroxide, showed no chlorine peaks. A sample of graphite was subjected to the reaction conditions, but EDS analysis indicated the absence of chlorine.

F. Infrared (IR) spectroscopy

The IR spectrum showed new peaks at 1155 and 1209 cm^{-1} [Fig. 6(c)] that are in the region of the C–C single bond stretch after treatment with dichlorocarbene. The IR spectrum showed two new peaks at 2851 and 2922 cm^{-1} after Birch reduction [Fig. 6(b)], typical of the C–H stretch in saturated hydrocarbons. The chemical analysis shows incorporation of nitrogen into the SWNTM during Birch reduction. Thus, the C–H stretching vibrations could arise from ethylenediamine

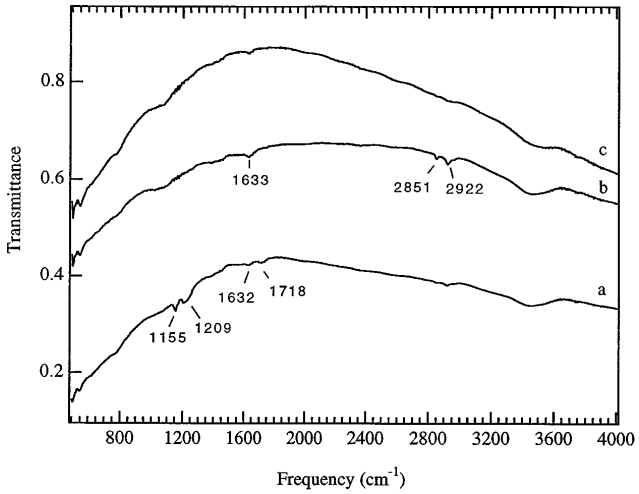

FIG. 6. IR spectra of SWNTM samples: (a) pristine, (b) after Birch reduction, and (c) after dichlorocarbene reaction (SWNTM2; SWNTM1 samples gave similar results).

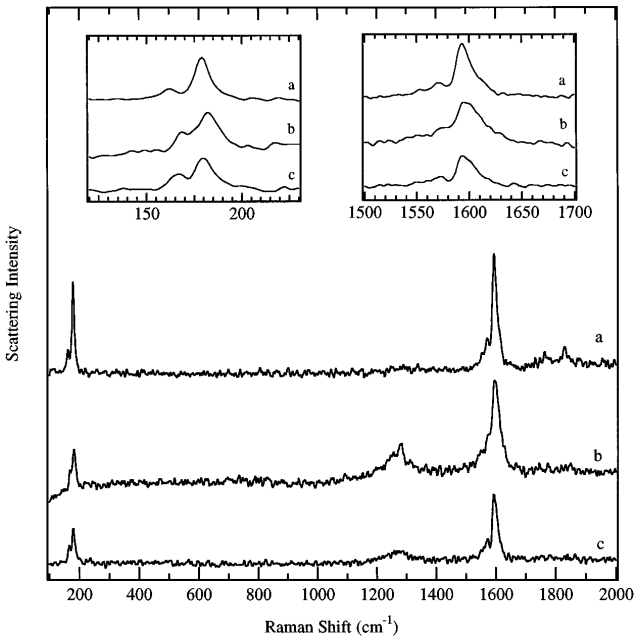

FIG. 7. Raman spectra of SWNTM samples: (a) pristine, (b) after treatment with Li/ethylenediamine, (c) after dichlorocarbene reaction (SWNTM1; SWNTM2 gave similar results).

molecules or fragments that have been incorporated into the SWNTM during reaction.

G. Raman spectroscopy

As discussed previously, the distinctive features of the Raman spectrum for SWNTM1 (and SWNTM2) include two strong first-order bands and several much weaker first- and second-order bands.[23] Using Nd:YAG excitation (1064 nm), two strong bands are observed, centered near 180 cm^{-1} and 1593 cm^{-1}. The band at 180 cm^{-1} has been identified with the A1g symmetry radial breathing modes, and the band at 1593 cm^{-1} has been assigned to an unresolved Raman triplet identified (in armchair symmetry tubes) with tangential carbon displacement modes, A1g, E1g, and E2g. These three, nearly degenerate, high frequency tubule phonons are related to the graphite E2g symmetry intralayer mode at 1582 cm^{-1}. The SWNT Raman bands, particularly the one identified with the radial breathing mode, are inhomogeneously broadened due to the tube diameter distribution.[23] Furthermore, the Raman scattering process has been shown to be resonant, and as the electronic bandstructure is sensitive to the diameter and chirality of the tubes, the Raman spectra depend noticeably on the excitation wavelength.[23] Thus, it was concluded[23] that different diameter and symmetry tubes are emphasized in the Raman spectrum, depending on the excitation wavelength.

In Fig. 7 we display room temperature Raman spectra for pristine SWNTM labeled (a) for pristine SWNTM1, (b) for the same batch of tubes after Birch reduction, and (c) for the same batch of tubes after reaction with dichlorocarbene. Only the strong bands discussed above can be seen in the spectrum of the pristine tubes (a). The Raman spectra for tubes exposed to Birch reduction conditions (b), and tubes reacted with dichlorocarbene (c), both exhibit a new broad peak centered near 1250 cm^{-1}. We interpret the presence of the broad peak in the Raman spectra of Figs. 7(b) and 7(c), as evidence for chemically induced disruption in the hexagonal carbon order in the nanotube wall. It should be noted that bands identified with C–H bend in sp^3 carbon are typically found in the region 1300–1450 cm^{-1}, yet there is no clear sign of these modes in Fig. 7(b), perhaps because their cross section is small. If chemical addition to the tube wall occurs in an ordered fashion, narrow, weak lines are expected in the Raman and IR spectra, depending on the symmetry and fraction of the tubes that have been functionalized. No new sharp lines are observed above the noise in the spectra. It is also interesting to note that the chemical treatment has substantially changed the intensity ratio R of the band at ~1593 to that of the band at 180 cm^{-1}. For the three spectra in Fig. 7 we find $R = 1.2:1$ (a; pristine), $R = 2:1$ (b; Birch), and $R = 1.8:1$ (c; dichlorocarbene). This change in R indicates a change in the electronic character of some of the tubes—presumably those outer tubes in the bundle that are most likely to interact with the reagents.

The insets in Fig. 7 show the two first-order-allowed strong bands at ~180 cm^{-1} and ~1593 cm^{-1} on an expanded frequency scale. Consistent with the appearance of a disorder-induced peak in the Raman spectra of the chemically treated tubes, these samples also exhibit a small increase in the linewidth of the first-order bands,

suggesting that functionalization of some of the tubes may have occurred.

H. High resolution transmission electron microscopy

In Figs. 8(a) and 8(b) we show SWNT's (SWNTM1), before and after reaction with dichlorocarbene. After inspection of many samples, we see no systematic difference between the pristine and reacted SWNT's. The amorphous carbon coating on the walls of the SWNT's is obvious in both cases.

III. DISCUSSION

The results are consistent with the incorporation of chemical functionalities into single-walled carbon nanotube material (SWNTM). Furthermore, the added functionality is not removed by washing with organic solvents or water.

The photolabeling studies show that the label is incorporated in the absence of photolysis. The presence of transition metal catalyst and amorphous carbon in the SWNTM may be sufficient to induce decomposition of the azides to nitrenes and to provide sites of high reactivity. Thus, it is clear that incorporation of the photolabel occurs by pathways other than the normal photochemical route in the case of the SWNTM.

The dichlorocarbene reaction induces strong changes in the XPS spectrum of the SWNTM, and chemical and EDS analyses show the presence of chlorine in the final sample. The chlorine seems to be localized fairly close to the surface of the SWNTM as it is easily removed by argon ion etching. Furthermore, the condensed mode EDS measurements show that some of the chlorine is associated with the SWNT bundles (but not with catalyst nanoparticles). The complicating factor is the presence of amorphous carbon on the walls of the SWNT. Thus we cannot say whether the chlorine is associated with the walls of the SWNT's or the amorphous carbon that is present on the walls at the start of the reactions.

The incorporation of nitrogen into the samples on reaction with Li/ethylenediame suggests that amide functionalities can also be added to the SWNTM.

The Raman and IR spectrum are consistent with small changes in the structure of the SWNT's, but do not unequivocally demonstrate that the dichlorocarbene or Birch reductions have actually modified the walls of the SWNT's. It seems that the bulk of the SWNT's are untouched by the chemical treatment.

In conclusion, our results are consistent with the addition of chemical functionalities to the surface of the SWNT bundles, but we cannot distinguish between attachment to the walls of the SWNT's and attachment to the amorphous carbon that is present on the walls in current samples.

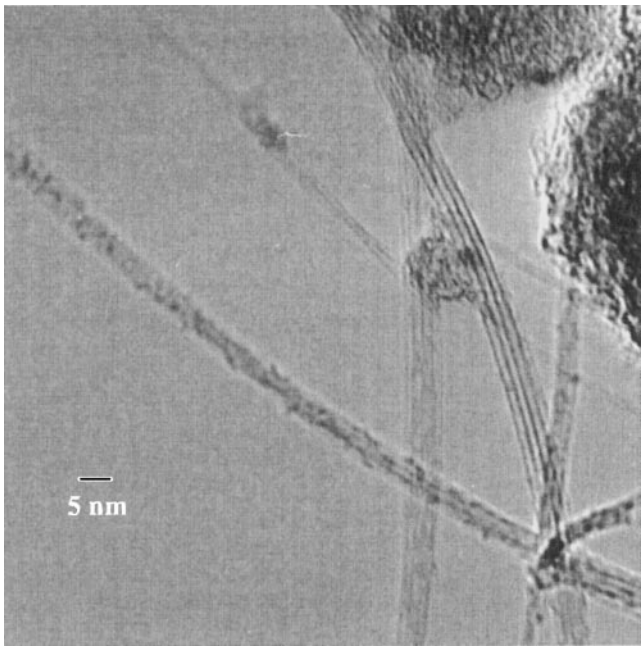

(a)

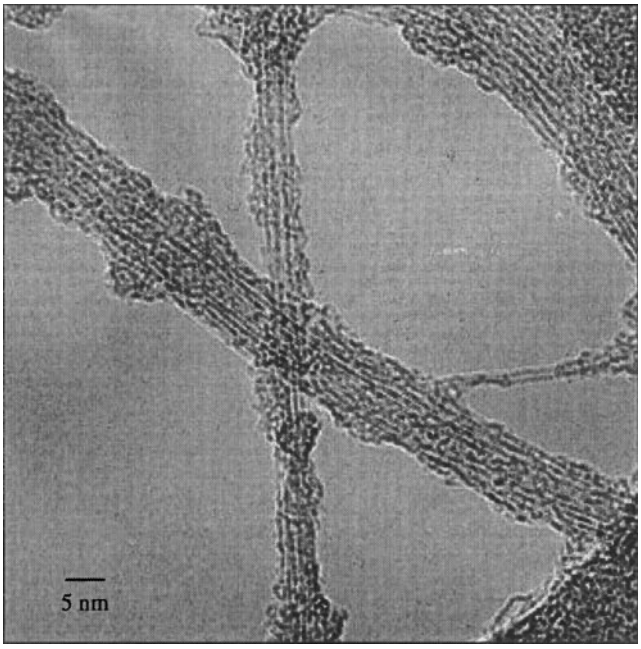

(b)

FIG. 8. (a) HRTEM image of pristine SWNTM samples (SWNTM1). (b) HRTEM image of SWNTM sample after reaction with dichlorocarbene (SWNTM1).

IV. EXPERIMENTAL

A. Photolabeling

A small amount of SWNTM sample (<1 mg) was dispersed in methanol (~0.5 ml) by vortexing and sonication (5 min). After addition of an aliquot (20 μl, 104 μm) of stock γBPA, the sample was vortexed for

https://doi.org/10.1557/JMR.1998.0337

5 min. The sample was photolyzed at 254 nm (hand held uv lamp, 6100 μW at 1 cm) for 15 min at room temperature with sonication. The mixture in the microcon was then centrifuged at 13,600 $\times$ *g* for 15 min at 4 °C to separate the unbound photoprobe from the nanotubes which were retained on the filter. The flow (as the first washing) though the filter was scintillation counted with Cerenkov method to determine the level of γ^{32}P. The nanotube sample was then resuspended in methanol (1.0 ml) by vortexing/rocking (5 min) at room temperature. The same centrifugation treatment as above served to separate the nanotube sample in the second washing. This washing procedure was repeated several times. The radioactive count was taken for all of the washings and the SWNTM under the same conditions. Consistent results were obtained on samples of SWNTM1 and SWNTM2, which gave essentially the same result. The photoprobes (adenosine 5′-[γ ^{32}P] triphosphate [γ] benzophenone and Guanosine 5′-[γ ^{32}P] triphosphate[γ] 4-Azidoanilide) were obtained from Affinity Labelling Technologies Inc., A215 ASTeCC Building, University of Kentucky, Lexington, KY 40506.

B. Chemical functionalization

1. Reaction with dichlorocarbene

In a typical experiment, 24.5 mg of pristine SWNTM's were mixed with chloroform (30 ml), water (20 ml), and phase transfer catalyst (PTC, triethylbenzylammonium chloride) (20 mg). After the mixture was sonicated for 4 h, NaOH (20 g) and chloroform (30 ml) were added. The mixture was stirred for 24 h. A white solid (NaCl) precipitated during the course of the reaction. PTC (20 mg), chloroform (30 ml), and a solution of NaOH (20 g in 20 ml water) were added again and the mixture was refluxed for 24 h. After the mixture cooled to room temperature, it was poured into a mixture of chloroform (100 ml) and water (200 ml) and shaken well and left standing for some time. The water and most of the chloroform were discarded directly, because the SWNTM's were suspended in the chloroform layer at the interface between the two layers. Water and chloroform were twice added to wash the sample. Hexane was then added and the organic layer washed with water and ethanol several times. Filtration with a Magna nylon membrane (pore size 0.45 μm) allowed the collection of the reacted SWNTM's on the membrane. The solid on the membrane was washed well with chloroform, ethanol, water, ethanol, and ether and then dried under vacuum for 24 h to yield 12 mg of product. Elemental analysis of two samples from this preparation gave C, 63.22%; H 0.86%; Cl, 5.15% (SWNTM1), C, 60.08%; H 1.75% Cl, 4.37% (SWNTM2).

2. Birch reduction (1)

SWNTM2 (19.5 mg) was placed in a three neck flask under argon. Liquid ammonia (~100 ml) was then trapped with a dry ice-acetone cooling bath into the flask. Lithium (0.54 g) was added in several portions with stirring. The mixture was stirred at −78 °C for 24 h and then refluxed for 36 h with a dry ice-acetone condenser. After a mixture of ethanol (20 ml) and ether (20 ml) was slowly added (1 h) at −78 °C, stirring was continued at −78 °C for 5 h. The cooling bath was removed and the stirring continued for 24 h to allow the ammonia to evaporate. Water (50 ml) and ether (50 ml) were then added to the flask. After stirring for 1 h, the mixture was filtered through a membrane (above) and the solid washed well with water, ethanol, and ether. The SWNTM's were then teased off the membrane as a single film (23.2 mg) and dried under vacuum for 24 h.

3. Birch reduction (2)

SWNTM1 (18 mg) was placed in a three-neck flask charged with ethylenediamine (50 ml) under argon. Lithium (0.30 g) was added in several portions with stirring at 100 °C. The mixture was stirred at 100 °C for 24 h and then ethylenediamine (50 ml) was added again. The mixture was stirred for another 24 h at 100 °C. After cooling to room temperature, stirring was continued and a mixture of water (10 ml) and ether (10 ml) was added dropwise (1 h) at room temperature, followed by a mixture of water (100 ml) and ethanol (100 ml). The mixture was sonicated for 5 min and centrifuged at 12,000 rpm. After decanting away the supernatant liquid, the residue was sonicated with water and again with ethanol. Membrane filtration (above) served to collect the SWNTM. The washing was repeated twice and the final product was dried under vacuum at room temperature to yield 50 mg of product (see text). Elemental analysis of a sample from this preparation gave C, 46.22%; H, 2.71%; N, 8.32%; F, 8.32%.

C. X-ray photoelectron spectroscopy

The samples were mounted on the spectrometer probe tip by means of double-sided adhesive tape. Spectra were obtained on a Kratos XSAM 800 spectrometer with Mg K_α (1.25 eV) radiation. The system pressure was maintained below 5×10^{-9} Torr using an ion pump and Ti sublimation pump to minimize contamination from vacuum contaminants. The spectrometer was run in fixed retarding ratio (FAT) mode at a pass energy of 12 kV and 14 mA. Under these conditions, the full-width at half-maximum (FWHM) of the Ag ($3d_{5/2}$) peak occurs at about 1.1 eV. The analyzer work function was determined by assuming a BE for Ag ($3d_{5/2}$) peak of 368.2 eV. It has been shown that the BE of C($1s$) from adventitious carbon on the standard Ag sample

surface is 285 eV when the silver $3d_{5/2}$ peak is taken as reference. For sample charging, all BE's were referenced to the C(1*s*) peak. Atomic concentrations were estimated from the XPS element peak area after applying atomic sensitivity factors.

Argon ion sputtering was carried out using a differentially pumped and computer-controlled 3M minibeam ion gun. The incident ion gun was operated at 3.5 keV, and sample currents were maintained at about 5.5 μA across a sample area. The pressure in the main chamber was maintained at about 5×10^{-7} Torr.

D. Transmission electron microscopy (TEM)

The microscopy was carried out with a 200 kV Philips CM200 instrument which was fitted with an Oxford Instruments light-element detector, and EMISPEC software was used for the analysis. In order to obtain EDS spectra of single ropes, the electron probe was condensed to approximately 10 nm.

E. Raman scattering

Raman scattering measurements were carried out in a backscattering geometry using Nd:YAG (1064 nm) laser excitation. The spectra were collected on a BOMEM Model DA3$^+$ Fourier transform instrument with a spectral slit width of $\sim$2 cm^{-1}.

ACKNOWLEDGMENTS

The synthetic and chemical studies on SWNT's were sponsored by NSF-EPSCoR Grant EPS-9452895.

The transmission electron microscopy studies were sponsored by the Division of Materials Sciences, U.S. Department of Energy, under Contract DE-AC0596OR22464 with Lockheed Martin Energy Research Corporation, and through the ShaRE Program under Contract DE-AC05-76OR00033 with Oak Ridge Associated Universities.

REFERENCES

1. B. I. Yakobson and R. E. Smalley, Am. Scientist **85**, 324–337 (1997).
2. R. S. Lee, H. J. Kim, J. E. Fischer, A. Thess, and R. E. Smalley, Nature (London) **388**, 255–257 (1997).
3. A. M. Rao, P. C. Eklund, S. Bandow, A. Thess, and R. E. Smalley, Nature (London) **388**, 257–259 (1997).
4. F. Wudl, Acc. Chem. Res. **25**, 157–161 (1992).
5. R. Taylor and D. M. R. Walton, Nature (London) **363**, 685 (1993).
6. A. Hirsch, *The Chemistry of the Fullerenes* (Thieme, Stuttgart, 1994).
7. F. Diederich and C. Thilgen, Science **271**, 317–323 (1996).
8. M. S. Meier, G-W. Wang, R. C. Haddon, C. P. Brock, M. L. Lloyd, J. P. Selegue, J. Am. Chem. Soc. **120**, 2337–2342 (1998).
9. R. C. Haddon, Science **261**, 1545–1550 (1993).
10. R. C. Haddon, J. Am. Chem. Soc. **119**, 1797–1798 (1997).
11. R. C. Haddon, G. E. Scuseria, and R. E. Smalley, Chem. Phys. Lett. **272**, 38–42 (1997).
12. P. M. Ajayan and S. Iijima, Nature (London) **361**, 333–334 (1993).
13. P. M. Ajayan, T. W. Ebbesen, T. Ichihashi, S. Iijima, K. Tanigaki, and H. Hiura, Nature (London) **362**, 522–523 (1993).
14. S. C. Tsang, P. J. F. Harris, and M. L. H. Green, Nature (London) **362**, 520–525 (1993).
15. S. C. Tsang, Y. K. Chen, P. J. F. Harris, and M. L. H. Green, Nature (London) **372**, 159–162 (1994).
16. A. Thess, R. Lee, P. Nikolaev, H. Dai, P. Petit, J. Robert, C. Xu, Y. H. Lee, S. G. Kim, A. G. Rinzler, D. T. Colbert, G. E. Scuseria, D. Tomanek, J. E. Fischer, and R. E. Smalley, Science **273**, 483–487 (1996).
17. R. C. Haddon, T. Fukunaga, Tetrahedron Lett., 1191 (1980).
18. P. G. Collins, A. Zettl, H. Bando, A. Thess, R. E. Smalley, Nature (London) **278**, 100–102 (1997).
19. D. Seyfreth, Acc. Chem. Res. **5**, 65–74 (1972).
20. R. C. Haddon, S. V. Chichester, S. M. Stein, J. H. Marshall, A. M. Mujsce, J. Org. Chem. **52**, 711 (1987).
21. M. Tsuda, T. Ishida, T. Nogami, S. Kurono, M. Ohashi, Tetrahedron Lett. **34**, 6911–6912 (1993).
22. J. Osterodt, F. Vogtle, Chem. Commun., 547–548 (1996).
23. A. M. Rao, E. Richter, S. Bandow, B. Chase, P. C. Eklund, K. A. Williams, S. Fang, K. R. Subbaswamy, M. Menon, A. Thess, R. E. Smalley, G. Dresselhaus, and M. Dresselhaus, Science **275**, 187–191 (1997).
24. J. W. G. Wildoer, L. C. Venema, A. G. Rinzler, R. E. Smalley, and C. Dekker, Nature (London) **391**, 59–61 (1998).
25. T. W. Odom, J-L. Huang, P. Kim, C. M. Lieber, Nature (London) **391**, 62–64 (1998).
26. C. Journet, W. K. Maser, P. Bernier, A. Loiseau, M. Lamy de la Chappelle, S. Lefrant, P. Deniard, R. Lee, J. E. Fischer, Nature (London) **388**, 756–758 (1997).
27. G. Dorman and G. D. Prestwich, Biochemistry **33**, 5661–5675 (1994).
28. M. T. Shoemaker and B. E. Haley, Biochemistry **32**, 1883–1890 (1993).
29. B. Sankaran, A. J. Chavan, and B. E. Haley, Biochemistry (1996).
30. N. J. Turro, *Modern Molecular Photochemistry* (Benjamin, Menlo Park, NJ, 1978).
31. M. Yan, S. X. Cai, and J. F. W. Keana, J. Org. Chem. **59**, 5951–5954 (1994).
32. R. E. Haufler, J. Conceicao, L. P. F. Chibante, Y. Chai, N. E. Byrne, S. Flanagan, M. M. Haley, S. C. O'Brien, C. Pan, Z. Xiao, W. E. Billups, M. A. Ciufolini, R. H. Hauge, J. L. Margrave, L. J. Wilson, R. F. Curl, and R. E. Smalley, J. Phys. Chem. **94**, 8634–8636 (1990).